Power Electronic Systems
Laboratory

Proceedings of the 7th IEEE International Power Electronics and Motion Control Conference (ECCE Asia 2012), Harbin, China, June 2-5, 2012

Fast High-Temperature (250°C/500°F) Isolated DC and AC Current Measurement: Bidirectionally Saturated Current Transformer

B. Wrzecionko,
L. Steinmann,
J. W. Kolar

Eidgenössische Technische Hochschule Zürich
Swiss Federal Institute of Technology Zurich

2012 IEEE 7th International Power Electronics and Motion Control Conference - ECCE Asia
June 2-5, 2012, Harbin, China

Fast High-Temperature (250 °C / 500 °F) Isolated DC and AC Current Measurement: Bidirectionally Saturated Current Transformer

Benjamin Wrzecionko, Lukas Steinmann and Johann W. Kolar
Power Electronic Systems Laboratory
ETH Zurich
Physikstrasse 3, 8092 Zurich, Switzerland
Email: wrzecionko@lem.ee.ethz.ch
Phone: +41 (0) 44 632 53 21, Fax: +41 (0) 44 632 12 12

***Abstract*—In an increasing number of application areas and industry sectors, such as the automotive, aerospace, military or oil and gas industry, a trend towards higher ambient temperature rating from 85 °C upward for electrical machines and power electronic converters can be observed. To reduce the impact of high ambient temperatures on the power density, the interest in power electronic converters with SiC power semiconductors operated up to a junction temperature of 250 °C rises.**

The control of power electronic converters typically requires a precise, fast and robust current measurement. Analyzing current measurement concepts from the literature reveals that there is a lack of a current measurement systems, that are galvanically isolated and are able to measure dc and ac fast at high ambient temperatures of 250 °C. In this paper, a current measurement concept of a bidirectionally saturated current transformer is presented, that is able to measure dc and sinusoidal ac up to 1 kHz and 50 A at an ambient temperature of 250 °C with an relative error of 2.6% and less than 0.5% after initial calibration. Furthermore, a prototype is designed, built and used for experimental verification of the concept.

***Index Terms*—Current Measurement, Current Transformers**

I. Introduction

A trend towards higher ambient temperature rating from 85 °C upward for electrical machines and power electronic converters can be observed in an increasing number of application areas and industry sectors. The automotive industry with the growing interest in hybrid electric vehicles (HEVs) [1], [2], the aerospace or military sector with future ambitious expeditions to e. g. the Venus [3] or the oil and gas industry with the exploration of deeper reservoirs [4] can be given as examples.

Most actual power electronic converters feature Silicon (Si) power semiconductors and thus their junction temperature is subjected to an upper temperature limit between 150 °C and 175 °C [5] due to the high intrinsic charge carrier concentration of Si [6]. In order to effectively remove the heat dissipated by the power semiconductor switches and maintain a reasonable size of the cooling system and thus reduce the impact of the high ambient temperature on the power density, a sufficiently large temperature difference between the semiconductor junction and the ambient has to be maintained.

Bidirectionally Saturated Current Transformer	
Current Range	-50 .. 50 A
Current Frequency Range	0 .. 1 kHz
Measurement Frequency	50 kHz
Max. Op. Temperature	250 °C
Outer Diameter[1]	6.5 mm
Inner Diameter[1]	2.9 mm
Height[1]	5.5 mm

[1] Including secondary winding

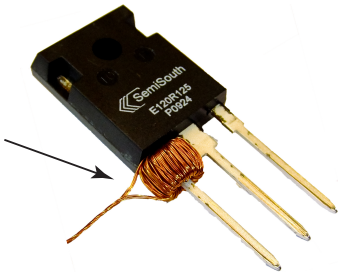

Fig. 1. Specifications and photograph of the bidirectionally saturated current transformer mounted on the terminal of a TO-220 packaged SiC JFET.

With Silicon Carbide (SiC), a new material that can be used for power semiconductor switches has become available. SiC switches are capable of significantly higher operating temperatures above 400 °C [7]. Novel joining and bonding technologies such as low-temperature sintered silver die attachment and copper bonding instead of aluminium bonding are currently investigated and promise considerably improved reliability for thermal cycling with increased temperature swing [8], [9].

Considering the example of an ambient-air-cooled power electronic dc-ac drive inverter for HEVs mounted under the engine hood [10], an ambient temperature of 120 °C can be assumed for the converter [1], [2]. To maximize the chip utilization and power density, a junction temperature around 250 °C for typical SiC power semiconductors at 120 °C ambient temperature has been shown to be close to the optimum junction temperature [11].

This means, also the signal electronics (including the current and voltage measurement), the passive components like dc-link capacitors as well as the components of the air-cooling system such as thermal interface materials, heat sinks and fans need to withstand these harsh temperature conditions. For the signal electronics and passives, a converter setup dealing with the challenges induced by 120 °C ambient and 250 °C junction temperature is shown in [10] where the signal electronics and passives are thermally shielded from the power semiconductors and remain at an ambient temperature level of

978-1-4577-2087-1/11/$26.00@2012 IEEE

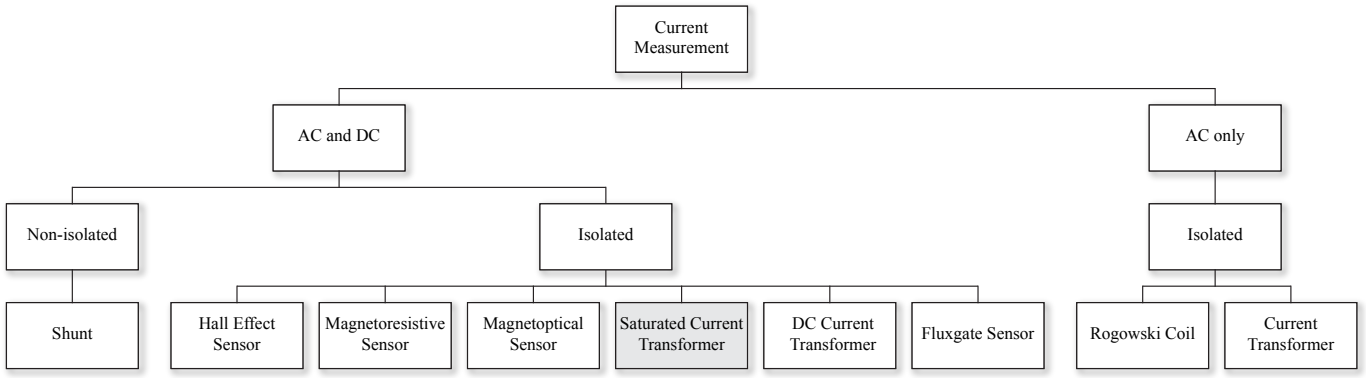

Fig. 2. Overview of state of the art current measurement concepts: For ac and dc measurement in high temperature applications, currently often shunts are used. Their measurement signal is not galvanically isolated, suffers from a temperature drift and can easily be distorted by EMI. For high ambient temperatures of 250 °C, Hall effect, magnetoresistive and magnetoptical sensors cannot be used due to individual technological temperature limits. Rogowski coils and current transformers can only measure ac down to a lower cut-off frequency. The concepts utilizing the magnetic flux in a coil or magnetic core caused by the current to be measured are generally more suitable for higher operating temperatures. The new concept introduced in this paper is the "Saturated Current Transformer", that is able to measure dc and sinusoidal ac up to 1 kHz and 50 A at an ambient temperature of 250 °C.

120 °C. Thermally conductive interface materials are available up to 300 °C [12], heat sinks are typically made of aluminum or copper and thus can withstand these temperatures as well. An automotive fan for operation at an ambient temperature of 250 °C, that offers a comparable fluid dynamic performance for power electronics cooling as the best-in-class conventional fans, is presented in [13].

For a high-quality control of a power electronic converter, ideally the current is measured precisely, robust against glitches, without any time lag and with a high bandwidth. To avoid letting the load current flow through the thermally shielded part of the signal electronics part, the current can be directly measured at the power semiconductor packages, and hence the measurement needs to withstand ambient temperatures of up to 250 °C [10]. Given the previous example [10], for the signal electronics that come possibly with a current measurement system, an ambient temperature capability of around 120 °C is sufficient if the control of the current measurement system can be separated from the actual measurement at the power semiconductors.

In recently published high temperature converter systems like [10], [14], the current is measured using shunts that operate at 250 °C. The analog-digital converter required for the digital control of the drive inverter can placed in the thermally shielded signal electronics box operating at 120 °C. Shunts offer an easy and cheap measurement of both dc and ac (raising the option of monitoring the dc drawn from the battery and the variable frequency ac output currents shaped by the inverter of an HEV using the same technology), but they are not galvanically isolated from the measured current and thus their voltage signal must be isolated if the shunt potential can be different from that of the signal processing electronics. Additionally, shunts require for accurate operation over large temperature ranges a temperature compensation due to the temperature drift of the resistance. Furthermore, the voltage measured at their terminals can easily be distorted by EMI occurring in switch mode power electronic converters, especially when mounted close to the power semiconductor switches. If the measured current ranges from small to very large currents, the value of the resistor has to be chosen sufficiently high so that small currents still lead to a measurable voltage across the resistor while at the same time, large currents at the opposite end of the measurement range will lead to high power losses and thus even higher temperatures in the resistor.

Alternative current measurement concepts are shown in Fig. 2. For high ambient temperatures of 250 °C, Hall effect, magnetoresistive and magnetoptical sensors cannot be used due to individual technological temperature limits. The concepts utilizing the magnetic flux in a coil or magnetic core caused by the current to be measured are generally more suitable for higher operating temperatures as the technology involved (windings and a ferro- or ferrimagnetic core) is available for these temperatures. Some of them suffer from other disadvantages: Rogowski coils and current transformers can only measure ac down to a lower cut-off frequency due to their operating principle based on the change of the magnetic flux. At low vehicle and thus rotational speeds of the electrical machine, the frequency of the output current in the range of less than 1 Hz is likely to be below the lower cut-off frequency of the coil or the transformer. A Fluxgate sensor can generally be used for dc and ac measurement at high temperatures, but the upper cut-off frequency of the sensor is very limited by the control of the saturable inductor sensing the magnetic flux of the gapped core.

In this paper, the novel current measurement concept of a "Bidirectionally Saturated Current Transformer" is presented, which allows fast measurement also of sinusoidal currents at high ambient temperatures of 250 °C for power electronic converters with medium switching frequencies and nearly sinusoidal output currents (e. g. due to a high load inductance). The introduced concept shares some common features with the dc current transformer that is known for many years

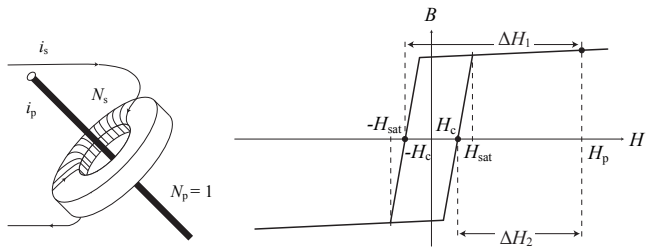

(a) (b)

Fig. 3. Basic physical setup of the bidirectionally saturated current transformer: The (primary) current i_p to be measured is fed through a toroidal core that also carries a secondary winding (a). Basic measurement principle: The primary current is determined using the mean value of the secondary currents that are needed to reach the coercive magnetic field strength $\pm H_\mathrm{c}$ of the hysteresis loop (b).

[15]–[17] but to make it suitable for measuring sinusoidal currents with frequencies of up to 1 kHz, it shows a modified magnetic design and is directly hardware controlled enabling significantly faster measurement than the usual dc measurement concepts and thus allowing to measure ac as well. The physical values measured to determine the current are also different to previously published concepts in order to eliminate any influence of the temperature. In the next Section II, the measurement principle, the differences to known concepts based on current transformers and the guidelines in choosing and dimensioning a core for this measurement system are shown in detail. Subsequently, the realization and experimental verification of a measurement system are presented in Section III and Section IV, respectively.

II. Measurement System

A. Measurement Principle

The basic physical setup of the current measurement system is shown in Fig. 4(a). The current i_p which is to be measured is fed through a toroidal core made of ferro- or ferrimagnetic material with N_p primary turns. Provided the magnetic permeability μ of the core is by orders of magnitude higher than that of the surrounding medium (e. g. air), the unknown primary current i_p that is to be measured causes a magnetic field strength that is given by

$$H_\mathrm{p} = \frac{i_\mathrm{p} \cdot N_\mathrm{p}}{l_\mathrm{m}} \tag{1}$$

where l_m denotes the average length of the magnetic path in the core. The core radius and the saturation magnetic field strength H_sat of the core material is chosen so small that the minimum current $i_\mathrm{p,min}$ that has to be measured leads to saturation of the core, i. e. to a value of $H_\mathrm{p} > H_\mathrm{sat}$.

As can be seen from Fig. 4(b), H_p can be calculated using the differences ΔH_1 and ΔH_2 in the magnetic field strength from H_p to the coercive magnetic field strength H_c:

$$H_\mathrm{p} = \frac{\Delta H_1 + \Delta H_2}{2} \tag{2}$$

The toroidal core also carries a secondary winding with N_s turns, driven by a full bridge (*cf.* Fig. 4(a)) causing a secondary current i_s and a secondary magnetic field strength H_s in the core. Hence, the magnetic setup should be viewed more as a two-winding inductor than an actual transformer. The H-bridge is controlled such that the full hysteresis loop is traversed within one pulse period of the H-bridge by the magnetic field strength H_s which is superimposed on H_p. During traversing the hysteresis loop, the currents i_s1 and i_s2 corresponding to $-H_\mathrm{c}$ and H_c, respectively, are measured using the shunt R_s and with

$$\Delta H_1 = \frac{i_\mathrm{s1} \cdot N_\mathrm{s}}{l_\mathrm{m}} \tag{3}$$

$$\Delta H_2 = \frac{i_\mathrm{s2} \cdot N_\mathrm{s}}{l_\mathrm{m}} \tag{4}$$

i_p can be finally calculated:

$$i_\mathrm{p} = \frac{N_\mathrm{s}}{N_\mathrm{p}} \cdot \frac{i_\mathrm{s1} + i_\mathrm{s2}}{2} \tag{5}$$

In Fig. 4(b) and (c), the idealized traversing of the hysteresis loop is shown in detail. The single phase inverter in Fig. 4(a) starts to apply the dc-link voltage V_cc to the secondary winding on the toroidal core at t_0. As the core is saturated by i_p and thus has got a relative permeability close to unity, the current i_s will rise fast.

Assuming the direction of i_s leads to a flux that is opposing the flux caused by i_p, the increase will become less steep once the sums of H_p and H_s add up to a value in between $-H_\mathrm{c}$ and H_c which happens at time instant t_1. At t_2, $i_\mathrm{s}(t = t_2) = i_\mathrm{s1}$ needs to be measured. With a further increase in i_s, the core will reach saturation again at t_3, leading to a steep increase in i_s until a predefined current limit is reached and the voltage applied to the secondary winding is reversed at t_4 and the hysteresis loop is traversed in the opposite direction, measuring $i_\mathrm{s}(t = t_6) = i_\mathrm{s2}$ and having $i_\mathrm{s}(t = t_9) = 0$ at t_9 where the switching period of the H-bridge starts again.

If the previous assumption that H_p and H_s are in opposite direction is wrong, the core will be saturated even further in the direction of H_p. Thus the current limit of i_s (either i_max or $-i_\mathrm{max}$) will be reached without desaturation of the core and thus also without any measurement of the secondary current and the H-bridge reverses the voltage so that the measurement cycle can start as described previously.

It can be seen in Fig. 4(c) that the time difference between t_7 and t_5 is smaller than between t_3 and t_1. The reason for this fact is illustrated in Fig. 5: When V_cc is applied to the secondary winding such that i_s rises (*cf.* Fig. 5(a)), the voltage drop caused by i_s across the parasitic resistances (drain-source on-resistance $R_\mathrm{DS,on}$ of the MOSFETs in the H-bridge and the winding resistance R_cu) and the shunt R_S reduce the voltage v_L applied to the secondary winding. Hence, it takes longer to build up the same inductor current, than it takes to make the inductor current decrease by applying V_cc in the opposite direction. This is true because i_s still flows in the same direction for both cases, but in the latter case, the voltage drop across the on-resistances of the other pair of switches and across R_s is added to V_cc and only the voltage drop across R_cu reduces v_L and thus the slope of i_s between t_1 and t_3.

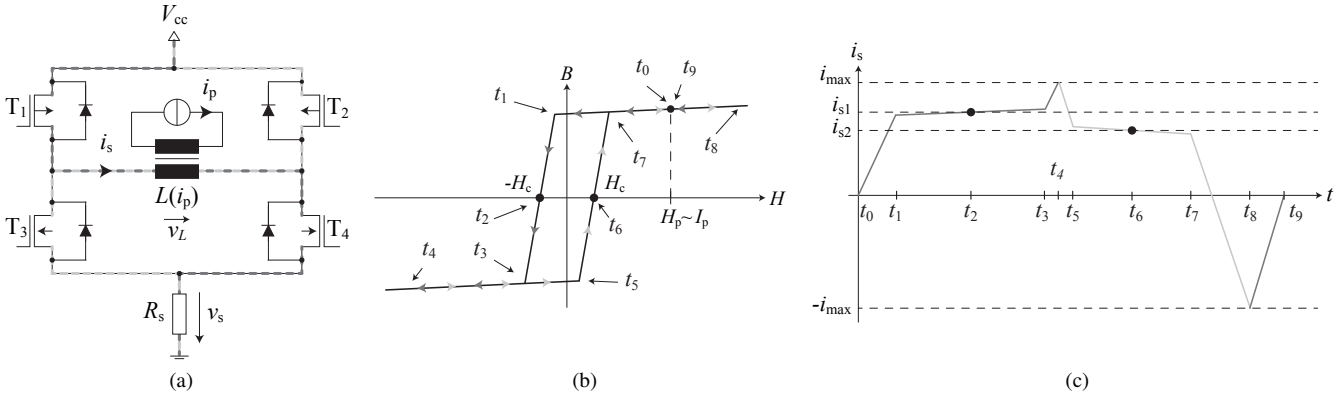

Fig. 4. Circuit diagram of the bidirectionally saturated current transformer including the primary current: The secondary winding on the toroidal core is connected to an H-bridge and the secondary current i_s is measured by a shunt R_s (a). Traversing the $B(H)$ hysteresis loop: The different operating points during one pulse period of the H-bridge are shown on the hysteresis loop (b) and the secondary current (c).

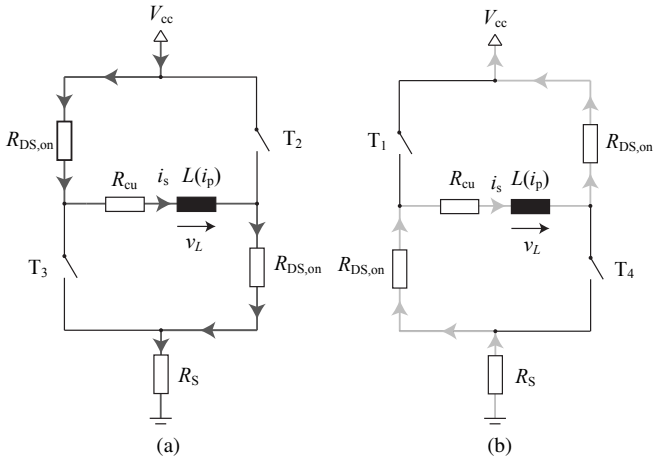

Fig. 5. Difference in inductor voltage depending on the switching state of the H-bridge: The direction of the secondary current i_s is independent of the switching state of the H-bridge for a given direction of the primary current during the time of a pulse period, when the core is not saturated. Hence, in one switching state (a), the voltage v_L applied to the inductor is V_cc less the ohmic losses occurring in $R_\mathrm{DS,on}$, R_s and R_cu and in the other switching state (b) v_L is V_cc less the ohmic losses in R_cu only. This leads to the fact that the time difference between t_7 and t_5 is smaller than between t_3 and t_1 in Fig. 4.

This phenomenon can also be explained by the following consideration: The shunt is in the dc-link, and the load is purely inductive, if losses are neglected. Hence, the current through (or voltage across) the shunt should the be free of a direct component. The second lowest waveform in Fig. 9 shows the shunt voltage for the secondary current as in Fig. 4(c). It can be seen, that the direct component in the shunt voltage v_s is introduced only by the difference in time that is spent in the region where the core is not saturated, and is finally caused by the losses in the parasitic resistances.

B. Major Differences to other Current Transformer Concepts

Measuring the secondary current at $\pm H_\mathrm{c}$ is a significant difference to [16] where the secondary current is measured when the core starts to saturate. The latter is difficult to realize with typical analog-digital-converters as the current rises very fast once the core is saturated. How the crucial task of finding the right point in time to sample the secondary current for the measurement principle presented in this paper can be tackled, is shown in Section III-D.

In [16], it is proposed to calculate the primary current by measuring the time to saturation. The saturation flux density, which shows a significant temperature dependence for typical ferro- or ferrimagnetic core materials (*cf.* e. g. the hysteresis loop in Fig. 6), is needed in the resulting equation for i_p though. It can be seen from (5) that the measurement of i_p in the concept shown in this paper is invariant against temperature changes of the core as N_s and N_p are temperature independent.

For an ideally lossless core material, the area enclosed by the hysteresis loop would be zero leading to $H_\mathrm{c} = 0$ and the difference in $i_{\mathrm{s}1}$ and $i_{\mathrm{s}2}$ would vanish. In reality, measuring $i_{\mathrm{s}1}$ and $i_{\mathrm{s}2}$ to find the mean value can lead to a more precise calculation of i_p using (5). Especially at measurement speeds resulting in high excitation frequencies, this is particularly important due to $|H_\mathrm{c}|$ increasing with frequency. Taking the width of the hysteresis loop into account when calculating the primary current is one important difference to [17].

C. Transformer Core

The choice of the transformer core material and design is crucial for the fast and precise operation of the current measurement system at ambient temperatures of 250 °C. It must be made sure, that the important material parameters mentioned in this section are assessed in the whole temperature range from -40 °C to temperatures above 250 °C as the core heats up to temperatures higher than the ambient temperature due to the losses occurring when traversing the hysteresis loop.

1) Relative Permeability μ_r: As shown in Section II-A, the sought current is determined by measuring the secondary current i_s at time instants t_2 and t_6, when the magnetic field strength in the core equals $\pm H_\mathrm{c}$. The increase in secondary current around H_c is small because the core is not saturated, hence its inductance value

$$L = \mu_\mathrm{r}\mu_0 N_\mathrm{s}^2 \cdot \frac{A_\mathrm{m}}{l_\mathrm{m}}, \tag{6}$$

where μ_0 is the magnetic constant and A_m is the cross section of the core, is proportional to the relative permeability μ_r. Hence, the slope of the secondary current

$$\frac{\mathrm{d}i_\mathrm{s}}{\mathrm{d}t} = \frac{v_L}{L} \tag{7}$$

can be reduced by increasing the relative permeability μ_r. This helps to decrease the measurement error, which is introduced if i_s is measured slightly too early or late.

2) Coercive Magnetic Field Strength H_c: In many other current measurement concepts utilizing two-winding inductors, the coercive magnetic field strength H_c causes a measurement error [17]. As pointed out in Section II-B, this error is compensated in the presented concept by measuring i_s1 and i_s2. Still, $|H_\mathrm{c}|$ should be chosen as small as possible in order to reduce the losses and thus the self-heating of the core when traversing the hysteresis loop.

3) Saturation Magnetic Field Strength H_sat: As explained in Section II-A, the core needs to be saturated for a precise measurement of the primary current. Hence, H_sat should be as small as possible as can be shown by

$$i_\mathrm{p} \overset{!}{>} i_\mathrm{p,min} = \frac{l_\mathrm{m}}{N_\mathrm{p}} \cdot H_\mathrm{sat}. \tag{8}$$

4) Saturation Flux Density B_sat: B_sat influences the time needed to traverse the full hysteresis loop and thus the measurement frequency f according to:

$$f = \frac{1}{\Delta t} = \frac{v_L}{\Delta B A_\mathrm{m} N_\mathrm{s}} \tag{9}$$

Assuming that it is not desired to provide a separate dc-dc converter for the current measurement system, v_L is given by V_cc, i. e. by the available voltage levels of the signal electronics. (Here, a value typical for the automotive industry of $V_\mathrm{cc} = 12\,\mathrm{V}$ is chosen.) Hence, for a fast current measurement, a small B_sat is desirable. The measurement frequency can also be adjusted using the product $A_\mathrm{m} N_\mathrm{s}$.

5) Number of Primary Turns N_p: It is desirable to design the measurement system such, that one primary turn $N_\mathrm{p} = 1$ is sufficient as this allows to position the core easily on the pin of a power semiconductor package (*cf.* Fig. 1).

6) Number of Secondary Turns N_s: For one primary turn, the number of secondary turns

$$N_\mathrm{s} = \frac{i_\mathrm{p}}{i_\mathrm{s}} \tag{10}$$

determines the level of the secondary current that is measured using the shunt R_s and needs to be switched by the H-bridge.

7) Core Cross Section A_m: A_m is inversely proportional to the measurement frequency as can be seen from (9) and hence should be chosen as small as manufacturing issues and the minimum required mechanical strength allow.

8) Length of the Magnetic Path l_m: According to (8), the length of the magnetic path l_m is directly proportional to the minimum current that can be measured and hence should be chosen as small as possible. Lower limits are introduced by the space consumed by the primary and secondary winding and by the mechanical strength of the core.

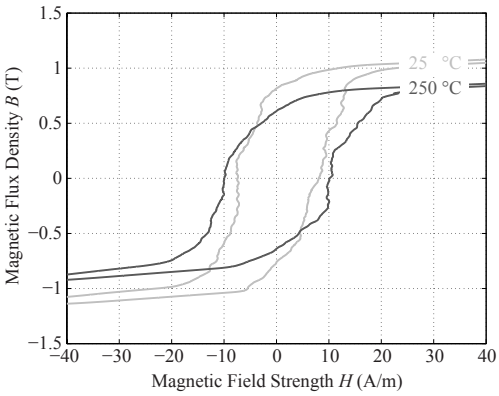

Fig. 6. Filtered hysteresis loop of "Vitroperm 500F" measured at 25 kHz and 25 °C and 250 °C using a "T60006-L2009-W914" core [18]. The material has been chosen because of a high μ_r up to 150'000, a low coercive and saturation magnetic field strength as well as a high operating temperature capability of up to 300 °C and a comparably high temperature invariance of these magnetic parameters. Furthermore, the commercial cores available are tape wound and hence, the core dimensioned can be easily adjusted to meet the needs of the experimental prototype of the bidirectionally saturated current transformer.

III. Realization of Measurement System

Having presented the working principle and important design parameters of the current measurement, in the following section the realized measurement system is described. The specifications of the realized systems include in addition to the temperature levels already mentioned in the introduction a current measurement range from -50 A to 50 A and a measurement frequency of at least 50 kHz for sinusoidal currents. The number of secondary turns is chosen to $N_\mathrm{s} = 50$ to limit the current in the H-bridge to 1 A. This allows a reasonable silicon chip size of the switches even at an ambient temperature of 120 °C (here, the two half-bridges are packaged each in an SO-8 package with an upper junction temperature limit of 175 °). Furthermore, it reduces the wire diameter needed for the secondary winding and thus helps to achieve a low l_m.

A. Choice of Core Material

The nanocrystalline material "Vitroperm 500F" is chosen for this example design as it features a high relative permeability up to $\mu_\mathrm{r} = 150'000$, a low coercive and saturation magnetic field strength as well as a comparably high temperature invariance of these magnetic parameters which is of great importance when designing a measurement system with a temperature difference during operation of more than 300 K (-40 °C to 250 °C ambient temperature plus self-heating due to losses). These characteristic values can be derived from Fig. 6 showing the hysteresis loop measured at 25 kHz (which matches the excitation frequency of the hysteresis loop for a measurement frequency of 50 kHz) and 25 °C and 250 °C using a "T60006-L2009-W914" core [18].

Even though the Curie temperature T_C of this material is higher than 600 °C, the manufacturer specifies an upper operating temperature limit of 155 °C for its "Vitroperm" core. This is primarily due to the epoxy coating or plastic casing of the cores. At temperatures above 300 °C, which

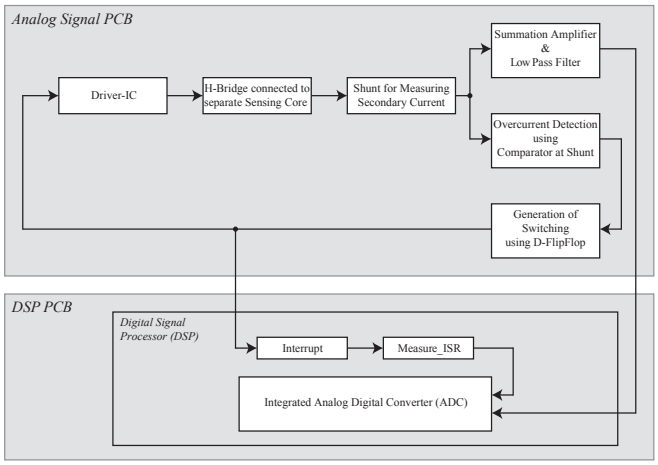

Fig. 7. Signal flow diagram for the analog control of the current measurement system and for the measurement routine within a DSP.

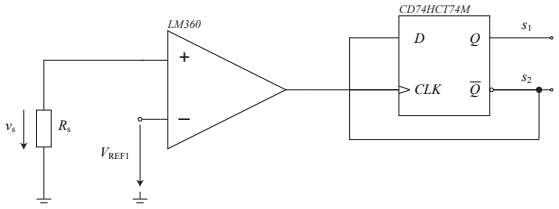

Fig. 8. Generation of switching signals for the H-bridge by comparing the shunt voltage with a reference voltage: The output of the comparator is fed to the clock input of a D flip-flop, the inverted output of which is connected to the D input of the flip-flop.

is still significantly below T_C, the material starts to loose its nanocrystalline structure resulting in derated performance especially with respect to eddy current losses and hence, it has to be made sure, that the material temperature does not rise significantly above 300 °C for a longer period of time.

B. Choice of Core Dimensions

The smallest commercially available "Vitroperm 500F" core ("T60006-L2009-W914", which has already been used for measuring the hysteresis loop in Fig. 6), has got a magnetic path length of $l_\mathrm{m} = 26\,\mathrm{mm}$ and a cross section of $A_\mathrm{m} = 6\,\mathrm{mm}$. This leads to undesirably high minimum current that can be measured and long time needed for traversing the hysteresis loop, as can be seen from (8) and (9), respectively.

The cores in the plastic casing can be opened and the tape wound core can be unwound and then re-wound with a smaller radius and less turns (leading to a lower l_m and A_m). For rewinding, the number N_t of "Vitroperm 500F" tape turns can be calculated using (9) to

$$N_\mathrm{t} = \frac{A_\mathrm{m}}{h_\mathrm{t} d_\mathrm{t}} = \frac{\Delta t v_L}{h_\mathrm{t} d_\mathrm{t} \Delta B N_\mathrm{s}} = 21 \qquad (11)$$

for $v_L \approx 11\,\mathrm{V}$ (V_cc is reduced by ohmic voltage drops), $\Delta B = 2.3\,\mathrm{T}$ (*cf.* Fig. 6) and $\Delta t = 20\,\mu\mathrm{s}$ (leading to a measurement frequency of 50 kHz due to the sampling scheme described in Section III-D), a height of the tape of $h_\mathrm{t} = 4.4\,\mathrm{mm}$ and a thickness of $d_\mathrm{t} = 20\,\mu\mathrm{m}$. This results in $A_\mathrm{m} = 1.9\,\mathrm{mm}^2$ and $l_\mathrm{m} = 13.8\,\mathrm{mm}$ and leads with (8) to a minimum measurable current of $i_\mathrm{p,min} = 0.28\,\mathrm{A}$ for $H_\mathrm{sat} \approx 20\,\mathrm{A/m}$ as a worst case scenario at 250 °C according to Fig. 6.

C. Signal Electronics

The structure of the signal electronics of the realized current measurement system is shown in Fig. 7: A PCB for the analog part containing the H-bridge and its gate-drivers is used to excite the core from the secondary side and a digital signal processor (DSP) mounted on a separate PCB samples at certain points in time (*cf.* Section III-D) the scaled (to fit the input voltage range of the analog-digital-converter (ADC) of the DSP) and filtered (by an active second order low pass filter) shunt voltage v_s. v_s itself and its scaled values (which correspond to the voltage v_ADC that is later filtered and applied to the ADC) are shown at the bottom of Fig. 9.

The switching signals (input signals of the gate driver) need to be generated very quickly after the core reaches saturation as the current rises very fast once it is saturated. Hence, they are not produced by the DSP but are generated by measuring the shunt voltage v_s and evaluating this voltage using a novel overcurrent detection circuit depicted in Fig. 8: The shunt voltage is compared to a reference voltage at a comparator. ($V_\mathrm{ref} = 0.64\,\mathrm{V}$ is chosen for this design, corresponding to a current through the $0.5\,\Omega$ shunt of 1.28 A making sure even with a maximum primary current of 50 A the secondary current can saturate the core in the direction opposing the primary current with $N_\mathrm{s} = 50$ turns.) The output of the comparator is fed to the clock input of a D flip-flop, the inverted output of which is connected to the D input of the flip-flop. Hence, every time the shunt voltage increases above V_ref, the rising clock edge makes the flip-flop toggle the output which is used as the switching signals for the n-MOSFET pairs T_1 and T_4 as well as T_2 and T_3.

D. Measurement Algorithm

The correct time instants to sample the shunt voltage are determined by the interrupt service routine "Measure_ISR", which is started by an interrupt generated by the output toggling of the flip-flop. Right at the start of the routine, a timer is re-started to measure the time until the next interrupt occurs. After half of the time that was started to be measured two interrupts before has elapsed, the middle of the interval, when the core is not saturated, is found and the ADC samples the shunt voltage (*cf.* Fig. 9). Hence, a measured current value can be provided twice per switching cycle of the H-bridge, e. g. twice per bidirectional traversing of the hysteresis loop.

Of course, this way of determining the point $(\pm H_\mathrm{c}, 0)$ in the H-B-plane works very precise only if the current does not change significantly within the interval between 3 interrupts. As an interrupt occurs in the current design every 7 μs to 14 μs and the maximum frequency of the sinusoidal currents that are to be measured is 1 kHz, only very small errors are introduced (*cf.* Section IV). Furthermore, at the beginning of the current

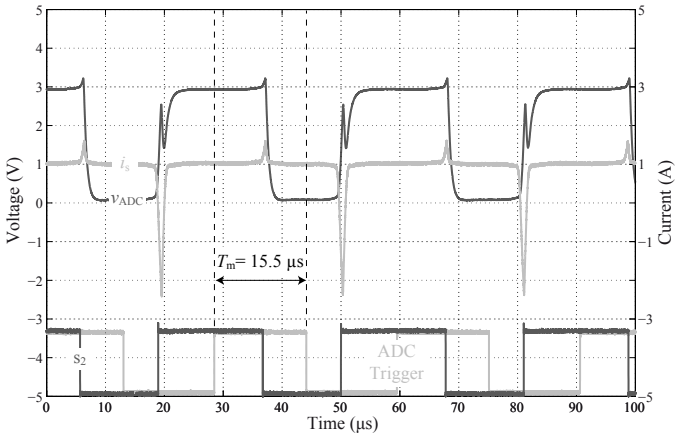

Fig. 10. Measured waveforms at 250 °C ambient temperature of the core: voltage v_{ADC} at the ADC of the DSP, shunt current i_{s}, switching signal s_2 and the software trigger starting the ADC conversion. The signals look as expected from the theoretical considerations in Fig. 9. Every 15.5 μs, corresponding to a measurement frequency of 67 kHz, a new current value is calculated.

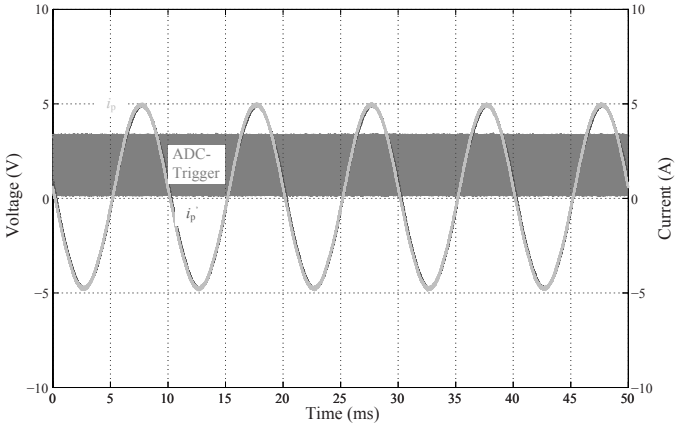

Fig. 11. The primary current measured with a wide band power analyzer and with the presented bidirectionally saturated current transformer.

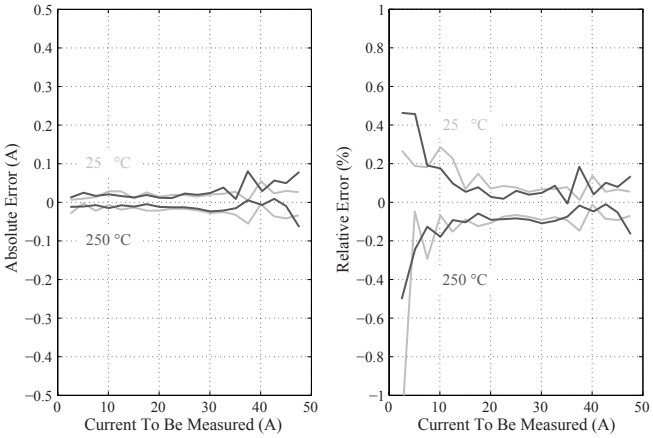

Fig. 12. Absolute (a) and relative (b) measurement error of the bidirectionally saturated current transformer after this setup has been initially calibrated to compensate for the linearity error introduced by tolerances of resistance values.

measurement (e. g. during start-up of the power electronic converter), the routine needs 1.5 pulse periods of the H-bridge ($\approx$ 50 μs) to initialize the variables where the counter values are stored in.

IV. Experimental Results

In this chapter, the theoretical considerations of the previous sections are experimentally verified using the realized measurement system of Section III. The waveforms shown in Fig. 9 can be directly compared with the waveforms in Fig. 10, measured at an ambient temperature around the core of 250 °C: The secondary current looks as expected, the ADC voltage is in the oscilloscope picture in Fig. 10 directly measured at the ADC inputs (i. e. after the low-pass filter which is used to avoid large voltage spikes on the signal) and the software trigger for starting the analog-digital conversion is shown in order to indicate the points in time when the shunt voltage is sampled. It can be seen that at 250 °C the software outputs an updated value of the measured primary current every 15.5 μs, corresponding to a frequency of 67 kHz. At room temperature, this values decreases to 54 kHz due to the increasing saturation flux density B_{sat} of the core (*cf.* (9) and Fig. 6). Fig. 11 shows the measurement of sinusoidal ac.

The measurement error is determined by a reference measurement of the primary current using a wide band power analyzer ("D6100" by Norma) with a 0.03% precision shunt. The absolute error of the described system scales linearly with the measured current, starting from an absolute error of 0.065 A at a primary current of 2.5 A to an error of 1.2 A at 47.5 A. Hence, the relative error is constantly at around 2.5%. This error is mainly due to the use of resistors (for the shunt and voltage level adjustment of the shunt voltage for the ADC, *cf.* Section III-C) that have a tolerance of their resistance around 1% and parasitic resistances of PCB tracks: A 10 mm long and 1 mm wide track has got a resistance of 4.8 mΩ, corresponding to 1% of the shunt resistor value.

As the primary current is calculated using the difference of two shunt voltages, errors due to offsets of e. g. the operational amplifiers used cancel out to a large extent. Hence, the linear error can be compensated in the software. The resulting absolute and relative measurement errors are shown in Fig. 12.

V. Conclusion

In this paper, first the upcoming quest for high temperature power electronic converters and particularly for fast measurement of dc and sinusoidal ac is motivated. The measurement principle of a novel concept called "bidirectionally saturated current transformer" is explained in detail, that is able to measure dc and sinusoidal ac up to 1 kHz and 50 A at an ambient temperature of 250 °C.

The important design guidelines for choosing a core material (high μ_{r}, low H_{c}, H_{sat}, B_{sat}) and the magnetic design (high N_{s}, low N_{p}, A_{m}, l_{m}) are derived and an experimental

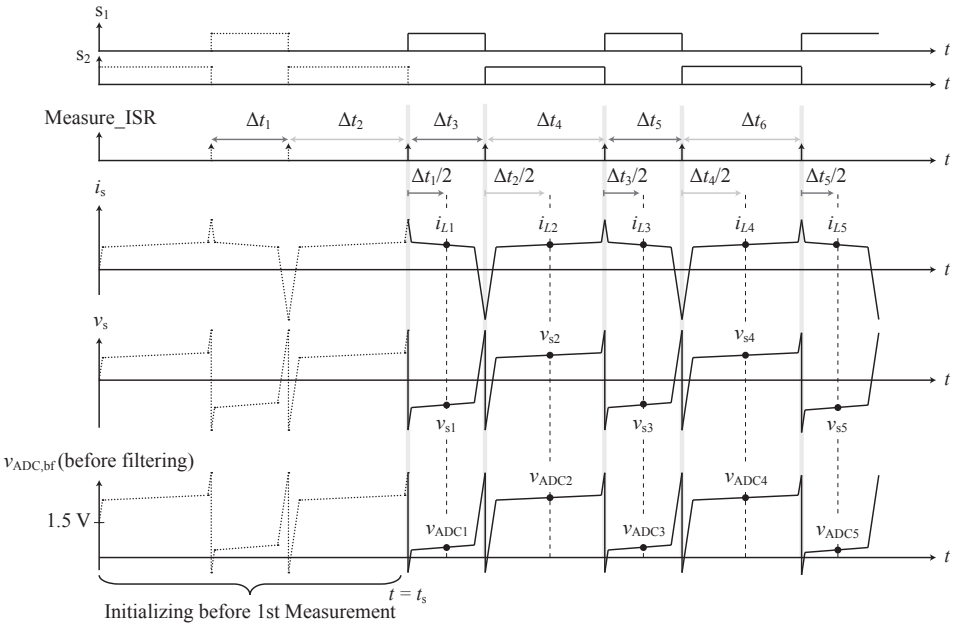

Fig. 9. The switching signals s_1 and s_2 generated by the circuit shown in Fig. 8 and the interrupts (visualized by vertical gray bars) triggering the DSP routine "Measure_ISR" to start the counters needed to determine the correct point in time when to sample the adjusted shunt voltage applied to the analog-digital-converter of the DSP are shown. Furthermore, the secondary current i_s of the bidirectionally saturated current transformer, the shunt voltage v_s and the voltage $v_{\mathrm{ADC,bf}}$ applied to a low-pass filter and then to the ADC.

prototype is designed accordingly. The required signal electronics consisting of an overcurrent detection that controls the H-bridge, which the secondary winding is connected to, and a circuit with a low-pass filter that also adjusts the voltage level of the shunt voltage which is sampled by the analog-digital-converter of a DSP. Finally, measurements verifying the proposed concepts are provided and show a relative error of 2.6% and less than 0.5% after calibration even at 250 °C.

REFERENCES

[1] F. Renken and R. Knorr, "High temperature electronic for future hybrid powertrain application," in *Proc. European Conference on Power Electronics and Applications (EPE 2005)*, Dresden, Germany, Sep. 11–14, 2005.

[2] S. Pischinger, M. Pischinger, H. Kemper, and S. Christiaens, "The challenges of system integration of the hybrid electric powertrain," in *Fachtagungsberichte VDE Kongress*, Aachen, Germany, Oct. 23–25, 2006.

[3] G. A. Landis, "Robotic exploration of the surface and atmosphere of Venus," *Acta Astronautica*, vol. 59, no. 7, pp. 570–579, 2006.

[4] A. König, "High temperature dc-to-dc converters for downhole applications," Ph.D. dissertation, RWTH Aachen University, Aachen, Germany, Jun. 2009.

[5] S. Matsumoto, "Advancement of hybrid vehicle technology," in *Proc. European Conference on Power Electronics and Applications (EPE 2005)*, Dresden, Germany, Sep. 11–14, 2005.

[6] B. J. Baliga, *Fundamentals of Power Semiconductor Devices*, Springer, Ed. Springer, 2008.

[7] T. Funaki, J. C. Balda, J. Junghans, A. S. Kashyap, H. A. Mantooth, F. Barlow, T. Kimoto, and T. Hikihara, "Power conversion with SiC devices at extremely high ambient temperatures," *Power Electronics, IEEE Transactions on*, vol. 22, no. 4, pp. 1321–1329, Jul. 2007.

[8] J. G. Bai, J. Yin, Z. Zhang, G.-Q. Lu, and J. D. van Wyk, "High-temperature operation of SiC power devices by low-temperature sintered silver die-attachment," *Advanced Packaging, IEEE Transactions on*, vol. 30, no. 3, pp. 506 –510, Aug. 2007.

[9] E. Schulze, C. Mertens, and A. Lindemann, "Pure low temperature joining technique power module for automotive production needs," in *Proc. 6th International Conference on Integrated Power Electronics Systems (CIPS 2010)*, Nuremberg, Germany, Mar. 16–18, 2010, pp. 333–338.

[10] D. Bortis, B. Wrzecionko, and J. W. Kolar, "A 120 °C ambient temperature forced air-cooled normally-off SiC JFET automotive inverter system," in *Proc. 26th Annual IEEE Applied Power Electronics Conference and Exposition (APEC 2011)*, Ft. Worth, TX, USA, Mar. 6–10, 2011, pp. 1282–1289.

[11] B. Wrzecionko, J. Biela, and J. W. Kolar, "SiC power semiconductors in HEVs: Influence of junction temperature on power density, chip utilization and efficiency," in *Proc. 35th Annual Conference of the IEEE Industrial Electronics Society (IECON 2009)*, Porto, Portugal, Nov. 3–5, 2009, pp. 3834–3841.

[12] *Thermal Navigator*, HALA Contec GmbH & Co. KG, Alte Landstraße 23, 85521 Ottobrunn, Germany, Oct. 2010. [Online]. Available: http://www.hala-tec.com/mod_use/dokumente/Thermal-Navigator_en.pdf

[13] B. Wrzecionko, A. Looser, J. W. Kolar, and M. Casey, "High-temperature (250 °C / 500 °C) 19'000 rpm BLDC fan for forced air-cooling of advanced automotive power electronics," in *Proc. 37th Annual Conference of the IEEE Industrial Electronics Society (IECON 2011)*, Melbourne, Australia, Nov. 7–10, 2011, pp. 4162–4169.

[14] P. Ning, F. Wang, and K. D. T. Ngo, "250 °C SiC high density power module development," in *Proc. 26th Annual IEEE Applied Power Electronics Conference and Exposition (APEC 2011)*, Ft. Worth, TX, USA, Mar. 6–10, 2011, pp. 1275–1281.

[15] J. R. Leehey, L. Kushner, and W. S. Brown, "DC current transformer," in *Proc. 13th Annual Power Electronics Specialists Conference (PESC 1982)*, Cambridge, MA, USA, Jun. 14–17, 1982, pp. 438–444.

[16] D. Azzoni, W. Teppan, and M. Carpita, "An innovative low-cost, high performance current transducer for battery monitoring applications: Prototype preliminary results," in *Proc. International Power Conversion Intelligent Motion Conference (PCIM Europe 2009)*, Nuremberg, Germany, May 12–14, 2009, pp. 443–449.

[17] J. A. Houldsworth, "Purpose-designed ferrite toroids for isolated current measurement in power electronic equipment," in *Proc. 4th Annual Power Conversion International Conference (PCI 1982)*, San Francisco, CA, USA, Mar. 29–31, 1982, pp. 101–109.

[18] *Nanocrystalline Vitroperm EMC Products*, Vacuumschmelze GmbH & Co. KG, Grüner Weg 37, 63450 Hanau, Germany, 2010. [Online]. Available: http://www.vacuumschmelze.com/fileadmin/Medienbiliothek_2010/Downloads/KB/Vitroperm_EMV_EN_full.pdf